International Journal of Mechanical Sciences 85 (2014) 142–151

Contents lists available at ScienceDirect

International Journal of Mechanical Sciences

journal homepage: www.elsevier.com/locate/ijmecsci

Calibration of anisotropic yield criterion with conventional tests or biaxial test

Shunying Zhang [a], Lionel Leotoing [a,*], Dominique Guines [a], Sandrine Thuillier [b], Shun-lai Zang [c]

[a] LGCGM, INSA, UEB, 20 avenue des Buttes de Coësmes, 35708 Rennes Cedex, France
[b] University of Bretagne-Sud, EA 4250, LIMATB, F-56100 Lorient, France
[c] School of Mechanical Engineering, Xi'an Jiaotong University, No. 28, Xianning Road, Xi'an, Shaanxi, China

ARTICLE INFO

Article history:
Received 18 December 2013
Received in revised form
6 May 2014
Accepted 19 May 2014
Available online 26 May 2014

Keywords:
Plastic anisotropy
Yield criterion
Biaxial test
Material parameter identification

ABSTRACT

Bron and Besson yield criterion has been used to model the plastic anisotropic behavior of an aluminum alloy series 5000. The parameters of this anisotropic yield model have been identified by two different methods: a classical one, considering several homogeneous conventional experiments and an exploratory one, with only one biaxial test. On one hand, the parameter identification with conventional experiments has been carried out with uniaxial tensile and simple shear tests in different orientations to the rolling direction and with a hydraulic bulge test, all of them considered at three equivalent plastic strain levels. On the other hand, Bron and Besson yield function has also been calibrated with inverse analysis from only a cross biaxial tensile test, since it was shown that the strain distribution in the center of the cruciform specimen is significantly dependent on the yield criterion. The principal strains along a specified path in the gauge area of the cruciform specimen have been analyzed and the gap between experimental and numerical values was minimized. Finally the yield contours obtained with the two methods have been compared and discussed.

1. Introduction

Sheet metal forming represents a class of important processes widely used in the manufacturing industry. Sheet metals usually exhibit a plastic anisotropy due to previous thermo-mechanical processes like rolling and annealing. To optimize the numerical simulation of the forming processes, an accurate description of the plastic behavior is required. Within a phenomenological description of the mechanical behavior of sheet metals, yield functions and especially anisotropic ones are used to represent the initial anisotropy of the material. Many anisotropic yield models were proposed to describe the initial anisotropy and identified from the mechanical properties, such as Hill 1948 [1], Barlat [2] (Yld 2000-2d), Barlat [3] (Yld2004-13p/18p) yield models and Karafillis–Boyce [4]; a thorough review of these models is presented in [5]. The initial anisotropy description, coupled with hardening evolution, can lead to a good representation of the mechanical behavior over a large strain range, e.g. [6]. An alternative consists in taking into account anisotropy evolution, as proposed in [7]. To consider the plastic strain-induced anisotropy, Zang and Lee [8] carried out the eigen decompositions of the linear transformation tensors of Yld2000-2d yield model at different equivalent plastic strains. Such an approach with the variation of anisotropic coefficients is not considered in this study, where plastic anisotropy coefficients are considered constants, over the investigated strain range.

Yield functions can involve a high number of material parameters. The calibration of these parameters requires usually several mechanical tests with different loading paths. To guarantee the relevance of the parameter set, the number of experimental data should not be lower than the number of material parameters considered in the identification process. In the case of the classical analytical approach, the experimental values, such as initial yield stresses and plastic anisotropy coefficients, obtained from mechanical tests are used as discrete input data or sampling points. The yield function makes an interpolation in-between these sampling points. Ideally, if the model is able to represent the mechanical behavior of the material, the interpolation points of the yield function correspond to these sampling points precisely. The relevance of the yield contour is improved when increasing the number of sampling points, demanding an increase of experimental information. However, from an economical point of view, the number of tests should be as small as possible. It has been proposed in [5] that at least the following experimental data

* Corresponding author. Tel.: +33 2 23 23 83 76; fax: +33 2 23 23 87 26.

http://dx.doi.org/10.1016/j.ijmecsci.2014.05.020
0020-7403/

is required: three yield stresses (e.g. σ_0, σ_{45} and σ_{90}) and three anisotropic coefficients (e.g. r_0, r_{45} and r_{90}) obtained from the uniaxial tensile tests in different orientations to the rolling direction (RD); an equi-biaxial yield stress (σ_b) and a biaxial coefficient (r_b) from biaxial tensile test, usually hydraulic bulge test. As mentioned above, most of the previous works proposed identification based on the initial values of these data, measured at the elasto-plastic transition. For the classical Hill 1948 yield criterion [1], three values among the ones indicated above are needed to calibrate three parameters in the case of a plane stress state. For the same stress condition, four values are needed to determine Barlat yield criterion involving four parameters [9]. Aretz [10] identified eight parameters of Barlat yield model (Yld2003) [11] with all the above-mentioned input data. Another method [12] was also proposed to identify this eight parameter yield model; indeed, the bulge test was replaced by two plane strain tensile tests. The major stresses at plastic yielding were taken as the input data. With the two linear transformation tensors introduced by Barlat [2], yield models were developed to be more and more flexible, such flexibility being related to the increase of the number of material parameters. Barlat and co-authors [3] calibrated the yield function Yld2004-18p with all the above-mentioned data and with additional data: the initial yield stresses and anisotropic coefficients from uniaxial tensile tests along 15°, 30°, 60° and 75° to RD. Bron and Besson yield model [13], also based on two linear transformation tensors, was identified similarly with a total of 16 parameters. From 2000, Banabic et al. proposed a series of yield models, which are called BBC yield models. For the 8 parameter yield criterion BBC2005 [14] and 16 parameter BBC2008 [15], Banabic et al. used the same input data as the above mentioned Yld2003 and Yld2004-18p respectively.

However, Hu [16] pointed out that the initial yield stresses were difficult to determine accurately since there exist several definitions of initial yielding. Some works investigated the identification of material parameters considering not only the initial values but also values recorded at higher strains. To predict the earing phenomenon in drawing and ironing process, Barros et al. [17] made a comparison of Cazacu and Barlat yield model [18] identified either from initial yield values or from the ones at an accumulated plastic work of 20 MPa. It is clearly shown that the yield model identified at an accumulated plastic work of 20 MPa gives a better description of the material mechanical behavior than the one identified from the initial values. Wang et al. [19] also proposed a strain-dependent identification method by considering the variation trend of the material values at different plastic strain levels. Another approach without considering initial yield stress values consists in parameter identification over the temporal evolution of experimental data. Zang et al. [6] considered a combination of stress level in uniaxial tension, equi-biaxial tension and simple shear, both monotonic and Bauschinger tests, to identify Bron and Besson yield function. Bron and Besson [13] also proposed a similar identification strategy with the temporal evolution of stress levels in tensile tests, both on straight and U-notched samples. It can be concluded that due to the dispersion on initial yield stresses as well as the evolution of anisotropy with strain, considering only initial yield stresses does not give an accurate description of the mechanical behavior. In this paper, the experimental values were obtained at several plastic strain levels.

Recently, some works have been focused on parameter identification of yield functions from the biaxial tensile test. Green et al. [20] have performed cross biaxial test with seven different proportional strain paths, in order to identify the parameters of several yield functions, some of them could not be identified by uniaxial tensile test but only with biaxial test. The authors adjusted the parameters with an iterative procedure to optimize the predicted strength level of two arms of the cruciform sample. Teaca et al. [21] proposed to identify Ferron, Makkouk and Morreale (FMM) yield function parameters [22] by combining results of uniaxial tensile tests and cross biaxial test. However, only two parameters of the yield model were calibrated from the strain distribution in the central part of the cruciform specimen. The field measurement of the strain level was also used by Prates et al. [23] to identify Hill 1948 coefficients. Up to now and to the authors' knowledge, there is no published work that concerns the parameter identification of a complex yield model with only one cross biaxial tensile test.

In the present article, Bron and Besson yield model is used to investigate the plastic anisotropy of AA5086 sheets. This yield model is flexible enough since the anisotropy is represented by 12 parameters, in the form of two linear fourth order transformation tensors; i.e. 4 isotropic parameters and 8 anisotropic parameters in plane stress condition. In order to identify these parameters, with two different methods, the mechanical behavior of AA5086 sheets of 2 mm thickness is investigated with homogeneous tests, like tension and simple shear, both at different orientations to RD, and hydraulic bulging, and also with cross biaxial test; all these results are original ones. The first identification method is based on an analytical description of the homogeneous conventional experiments. The experimental values at different equivalent plastic strain levels are obtained from these tests as the input values. Hill 1948 yield function was also calibrated with these conventional results. It is shown that the numerical prediction of the strain distribution at the cruciform specimen center is significantly modified by the yield criterion. The second method relies on the cross biaxial tensile test and all parameters of Bron and Besson yield function are identified with a cruciform specimen since it is shown that the strain distribution in the central area of the specimen depends significantly on the yield criterion. Comparison between experimental and numerical results of principal strains along a specified path in the gage area of the cruciform specimen is performed. It is shown that the cross biaxial test involves a large range of strain paths, though the maximum strain is limited. Finally, the yield models identified by the two identification methods are compared.

2. Material model

Assuming orthotropic symmetry, $(\vec{1}, \vec{2}, \vec{3})$ are respectively the rolling direction (RD), the transverse direction (TD) and the normal direction (ND). In the frame of a uniaxial tensile test, $(\vec{x}, \vec{y}, \vec{z})$ are respectively the tensile direction, the transverse direction in the sheet plane and the normal direction.

2.1. Hill 1948 yield function

Hill 1948 orthotropic yield function is written in the following form [1]:

$$\psi_H = F(\sigma_{22}-\sigma_{33})^2 + G(\sigma_{33}-\sigma_{11})^2 + H(\sigma_{11}-\sigma_{22})^2 + 2L\sigma_{23}^2 + 2M\sigma_{13}^2 + 2N\sigma_{12}^2 \quad (1)$$

where ψ_H denotes the yield function. Plastic yielding occurs when $\psi_H = \overline{\sigma}^2 = Y_0^2$ where $\overline{\sigma}$ is the equivalent stress and Y_0 a reference yield stress of the material. F, G, H, L, M and N are material parameters. When the condition $G+H=1$ is imposed, Y_0 is the uniaxial yield stress along the rolling direction. Then, with plane stress condition ($\sigma_{33}=\sigma_{13}=\sigma_{23}=0$), three independent anisotropic parameters F, G and N have to be identified.

Hill parameters can be calculated from three anisotropic coefficients r_θ with $\theta=(\vec{x},\vec{1})=0^\circ,45^\circ,90^\circ$ that are defined by:

$$r_\theta=\frac{\dot{\varepsilon}^p_{yy}}{\dot{\varepsilon}^p_{zz}} \tag{2}$$

where $\dot{\varepsilon}^p_{yy}$ and $\dot{\varepsilon}^p_{zz}$ are the plastic strain increments along the transverse direction and the normal direction respectively. Hill parameters F, G and N are defined by

$$F=\frac{r_0}{r_{90}(r_0+1)},\quad G=\frac{1}{r_0+1}\quad\text{and}\quad N=\frac{(1+2r_{45})(r_0+r_{45})}{2r_{90}(1+r_0)} \tag{3}$$

2.2. Bron and Besson yield function

Bron and Besson proposed a yield function involving 16 parameters under the form [13]:

$$\psi(\sigma_{ij})=\left(\sum_{k=1}^{2}\alpha^k(\overline{\sigma}^k)^a\right)^{1/a} \tag{4}$$

α^k are positive coefficients, the sum of which is equal to 1. Plastic yielding occurs when $\psi=\overline{\sigma}=Y_0$ and $\overline{\sigma}$ and Y_0 have the same definitions as in Section 2.1. However, Y_0 is no longer equal to the uniaxial yield stress in the rolling direction. $\overline{\sigma}^k$, $k=1,2$ are expressed in the form:

$$\begin{aligned}\overline{\sigma}^1&=\left(\frac{1}{2}\left(\left|S^1_2-S^1_3\right|^{b_1}+\left|S^1_3-S^1_1\right|^{b_1}+\left|S^1_2-S^1_1\right|^{b_1}\right)\right)^{1/b_1}\\ \overline{\sigma}^2&=\left(\frac{3b_2}{2^{b_2}+2}\left(\left|S^2_1\right|^{b_2}+\left|S^2_2\right|^{b_2}+\left|S^2_3\right|^{b_2}\right)\right)^{1/b_2}\end{aligned} \tag{5}$$

a, b_1, b_2 and α^1 ($\alpha^2=1-\alpha^1$) are four isotropic parameters which define the shape of the yield surface. S^k_i are the principal values of the transformed stress deviators $s'_{ij}k$ defined by:

$$s'_{ij}k=L^k\sigma_{ij}$$

$$\text{with } L^k=\begin{pmatrix}\frac{c^k_2+c^k_3}{3} & -\frac{c^k_3}{3} & -\frac{c^k_2}{3} & 0 & 0 & 0\\ -\frac{c^k_3}{3} & \frac{c^k_1+c^k_3}{3} & -\frac{c^k_1}{3} & 0 & 0 & 0\\ -\frac{c^k_2}{3} & -\frac{c^k_1}{3} & \frac{c^k_1+c^k_2}{3} & 0 & 0 & 0\\ 0 & 0 & 0 & c^k_4 & 0 & 0\\ 0 & 0 & 0 & 0 & c^k_5 & 0\\ 0 & 0 & 0 & 0 & 0 & c^k_6\end{pmatrix} \tag{6}$$

where c^k_i are 12 parameters which are related to the anisotropy of the material. In plane stress condition, the anisotropic parameter number reduces to 8 with $c^k_5=c^k_6=1$.

3. Parameter identification of yield model with conventional tests

3.1. Material data

In this work, three uniaxial tensile tests (UT) along 0°, 45° and 90° according to the rolling direction, two simple shear tests (SS) along 0° and 45° and one bulge test have been considered to identify Bron and Besson yield model. Hill 1948 parameters were also identified from the three anisotropic coefficients for comparison's sake.

Material data used in the identification process corresponding to three uniaxial tensile stresses (σ_0, σ_{45} and σ_{90}) and three anisotropic coefficients (r_0, r_{45} and r_{90}), two simple shear stresses (τ_0 and τ_{45}), an equi-biaxial stress (σ_b) and a biaxial coefficient (r_b) are obtained at three different levels of the equivalent plastic strain $\overline{\varepsilon}^p$ ($\overline{\varepsilon}^p=0.02$, $\overline{\varepsilon}^p=0.05$ and $\overline{\varepsilon}^p=0.1$). The strain levels were selected according to the maximum strain range of the tests in the database (cf. Fig. 1).

3.2. Numerical calculation of material data

In the plane stress condition, σ_{11}, σ_{22} and σ_{12} are the only non-zero stress components. With the associated flow rule

$$\dot{\varepsilon}^p_{ij}=\dot{\lambda}\frac{\partial\psi}{\partial\sigma_{ij}} \tag{7}$$

plastic strain increments can be written as a function of the gradient of the yield function:

$$\dot{\varepsilon}^p_{ij}=\dot{\lambda}\begin{pmatrix}\frac{\partial\psi}{\partial\sigma_{11}} & \frac{\partial\psi}{\partial\sigma_{12}} & 0\\ \frac{\partial\psi}{\partial\sigma_{21}} & \frac{\partial\psi}{\partial\sigma_{22}} & 0\\ 0 & 0 & -\left(\frac{\partial\psi}{\partial\sigma_{11}}+\frac{\partial\psi}{\partial\sigma_{22}}\right)\end{pmatrix} \tag{8}$$

Assuming that the uniaxial tensile test is performed along a direction defined by an orientation angle θ from the rolling direction, then the anisotropic coefficient r^M_θ can be calculated by:

$$r^M_\theta=\frac{\dot{\varepsilon}^p_{yy}}{\dot{\varepsilon}^p_{zz}}=\frac{(\partial\psi/\partial\sigma_{11})sin^2\theta-(\partial\psi/\partial\sigma_{12})sin2\theta+(\partial\psi/\partial\sigma_{22})cos^2\theta}{(\partial\psi/\partial\sigma_{11})+(\partial\psi/\partial\sigma_{22})} \tag{9}$$

The biaxial coefficient r^M_b is calculated in the form:

$$r^M_b=\frac{\dot{\varepsilon}^p_{yy}}{\dot{\varepsilon}^p_{xx}}=\frac{(\partial\psi/\partial\sigma_{22})}{(\partial\psi/\partial\sigma_{11})} \tag{10}$$

As the identification process is performed with three levels of plastic equivalent deformation, the cost function δ_c is then defined by

$$\delta_c(Y_0{}^S,a,b_1,b_2,\alpha^1,c^k_i)=\sum_{S=1}^{3}\delta_S+\sum_{j=1}^{3}((r^M_{\theta_j}-r_{\theta_j})/r_{\theta_j})^2+((r^M_b-r_b)/r_b)$$

$$\text{with}\quad \delta_S=\sum_{j=1}^{3}((\sigma^{MS}_{\theta_j}-\sigma^S_{\theta_j})/\sigma^S_{\theta_j})^2+((\sigma^{MS}_b-\sigma^S_b)/\sigma^S_b)^2+\omega\sum_{j=1}^{2}((\tau^{MS}_{\theta_j}-\tau^S_{\theta_j})/\tau^S_{\theta_j})^2 \tag{11}$$

where r_{θ_j} and r_b are respectively experimental anisotropic coefficients and biaxial coefficients calculated as average values over an equivalent plastic strain range from 0.02 to 0.1; $r^M_{\theta_j}$ (Eq. (9)) and r^M_b (Eq. (10)) are predicted anisotropic coefficients and biaxial coefficients; $\sigma^M_{\theta_j}$, $\tau^M_{\theta_j}$ and σ^M_b are the predicted stress values at different plastic deformation levels. In Eq. (11), index S refers to the plastic strain levels whereas index j relates to the test orientation. Y^S_0,

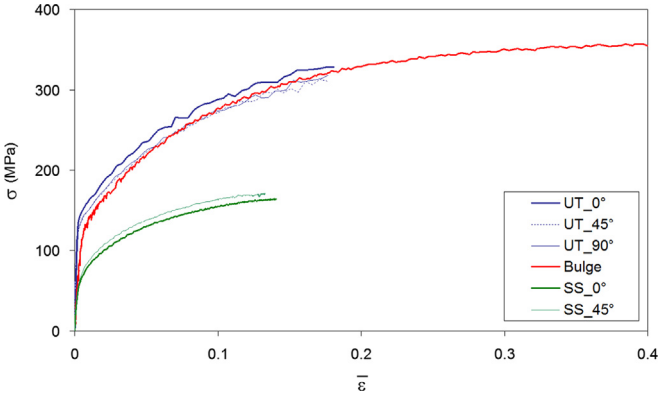

Fig. 1. Cauchy stress versus equivalent strain curves for conventional tests.

$S=1,3$, are the critical values, when yielding occurs, of the equivalent yield stress for the three equivalent plastic strains considered in the identification. ω is a weight coefficient introduced to change the relative importance of shear tests compared to tensile tests and bulge test in the optimization process. Indeed, the elasto-plastic transition in simple shear is particularly rounded, leading to an increased difficulty to determine the initial values of the yield stress in simple shear. Therefore, in order to reach a compromise between tension and simple shear, an optimum value of ω was determined by successive trials.

In case of anisotropy, as Y_0 is no longer equal to the uniaxial stress σ_0 along the rolling direction, it has to be identified along with the parameters related to anisotropy. There is therefore a total of 15 material parameters to be identified for Bron and Besson criterion. The major task lies in the optimization of the anisotropic parameters to minimize the cost function. The algorithm Broyden–Fletcher–Goldfarb–Shanno (BFGS) [24] is preferred here. BFGS is an approximate Newton's method, which is a hill-climbing optimization. The convergence is rapid but the optimized set strongly depends on the initial set. To overcome this difficulty and thanks to the efficiency of the algorithm, the optimization can be led with a large number of initial sets to cover all the parameter ranges. The identification process is realized with the commercial software modeFRONTIER® [25] which is an integration platform for multi-objective optimization. It provides a coupling with third party engineering software such as MATLAB to design an automatic simulation and simplify the analysis process.

3.3. Application for AA5086

The above-mentioned conventional tests have been performed for aluminum alloy 5086. The sheet thickness is 2 mm. Experimental curves in stress equivalent strain level for these tests are presented in Fig. 1. For all the tests, strains have been measured by the digital image correlation (DIC) method. These tests can be considered homogeneous, at least over a restricted area, and an average strain value was calculated over this area. Stresses have been directly calculated from measures of force (uniaxial tension and simple shear tests) or pressure (bulge test). The equivalent strain is defined by:

$$\bar{\varepsilon} = \sqrt{\frac{2}{3}\sum_{i,j}\varepsilon_{ij}^2} \tag{12}$$

It can be seen that necking limits the homogeneous equivalent strain in tension at around 0.2, whereas a maximum value of 0.4 in bulge test is reached. The low maximum equivalent strain reached in simple shear comes from premature failure of the sample under the grip, partly due to the relatively high material thickness (2 mm) that entails a rather high force for the clamping under the grips.

The anisotropic coefficients r_θ, obtained from uniaxial tensile tests, decrease with the plastic strain. This evolution is represented in Fig. 2, for two equivalent plastic strain ranges [0.02, 0.1] and [0.1, 0.15]. For each strain range, r_θ is calculated as the linear regression of the evolution of $\dot{\varepsilon}_{yy}^p$ as a function of $\dot{\varepsilon}_{zz}^p$ (Eq. (2)), over the considered strain range.

Experimental material data for AA5086 is given in Table 1. The stresses are determined at an equivalent plastic strain $\bar{\varepsilon}^p = 0.02$, $\bar{\varepsilon}^p = 0.05$ and $\bar{\varepsilon}^p = 0.1$ respectively for each test. The anisotropic coefficients (r_0, r_{45}, r_{90}) are the ones calculated for an equivalent plastic strain range from 0.02 to 0.1, in order to keep the same strain range as for the stress levels. It can be seen that this material does not exhibit the anomalous behavior [26], indeed r_θ are less than one and the biaxial stress σ_b is lower than the uniaxial tensile stress σ_0.

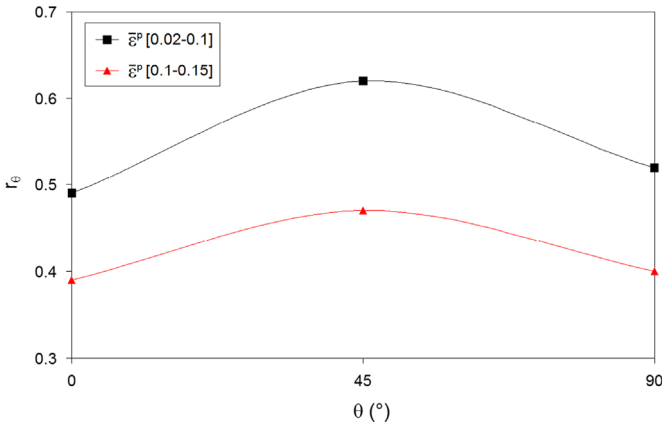

Fig. 2. Anisotropic coefficients calculated over two different equivalent plastic strain ranges.

Table 1
Material data derived from the conventional tests.

	σ_0 [MPa]	σ_{45} [MPa]	σ_{90} [MPa]	σ_b [MPa]	τ_0 [MPa]	τ_{45} [MPa]	r_0	r_{45}	r_{90}	r_b
$\bar{\varepsilon}^p = 0.02$	191	179	178	172	102	109	0.49	0.62	0.52	1.03
$\bar{\varepsilon}^p = 0.05$	239	228	226	226	131	139				
$\bar{\varepsilon}^p = 0.1$	290	276	276	284	156	164				

In the optimization process, a first step is to fix the variation range for the parameters. The range used in this work is given in Table 2. For Y_0, the variation range is set to be from $0.80\sigma_0$ to $1.20\sigma_0$, from several trials. Then one hundred initial parameter sets for the algorithm BFGS can be generated to cover the variation range of all the parameters.

The 13 parameters of Bron and Besson yield function calculated from the experimental data of Table 1 are given in Table 3. During the identification process, the weight coefficient ω is set equal to 0.5. Indeed, for higher values of ω, especially for the low value of the equivalent plastic strains, the predicted tensile results were too far from the experiments.

As a comparison, Hill 48 yield criterion has been calibrated by the three (r_0, r_{45}, r_{90}) values, from data given in Table 1, and are presented in Table 4.

Figs. 3–6 show the results for both Bron and Besson and Hill 1948 yield criteria. Both of them predict well the anisotropic coefficient evolution with θ. The experimental r-value is the one at plastic strain ranges [0.02, 0.1]. For the uniaxial yield stresses at three equivalent plastic strain levels $\bar{\varepsilon}^p = 0.02$, $\bar{\varepsilon}^p = 0.05$ and $\bar{\varepsilon}^p = 0.1$, Bron and Besson yield function gives also a good description, while Hill 1948 yield model has not the ability to follow their variations. For shear stresses, compared to Hill 1948 predictions, Bron and Besson predicted values are very close to the experimental ones at each strain level. The associated yield surfaces are presented in Fig. 6. The yield model predicts the biaxial stress perfectly but only at $\bar{\varepsilon}^p = 0.05$, it has a 4.8% overestimation at $\bar{\varepsilon}^p = 0.02$, while a 3.6% underestimation can be noticed at $\bar{\varepsilon}^p = 0.1$. For the r_b coefficient, as it can be observed for the r_θ coefficients (Fig. 3), the prediction is excellent.

During this identification process, the 13 parameters are computed by means of 10 input values, which are obtained from six experimental tests (3 UT, 2 SS, 1 Bulge). The insufficient input data may lead to non-unique sets of parameters. In this work, the set corresponding to the lowest value of the cost function was kept.

Table 2
Central values and variation ranges (in brackets) for each parameter.

α_1	a	b_1	b_2	c_1^1	c_2^1
0.5 (0.1∼0.9)	6 (0–12)	10 (0–20)	10 (0–20)	0.5 (−1.2 to 2.2)	0.5 (−1.2 to 2.2)
c_3^1	c_4^1	c_1^2	c_2^2	c_3^2	c_4^2
0.5 (−1.2 to 2.2)	0.5 (−1.2 to 2.2)	0.5 (−1.2 to 2.2)	0.5 (−1.2 to 2.2)	0.5 (−1.2 to 2.2)	0.5 (−1.2 to 2.2)

Table 3
Anisotropic parameters of Bron and Besson yield function identified from conventional tests. Three different values for Y_0 have been identified, corresponding to each equivalent plastic strain level.

$Y_0^S(MPa)$	α_1	a	b_1	b_2	c_1^1	c_2^1	c_3^1	c_4^1	c_1^2	c_2^2	c_3^2	c_4^2
196.0/245.2/297.5	0.13	3.39	16.17	7.34	1.69	1.70	1.19	1.41	0.97	0.79	0.98	1.01

Table 4
Parameters of Hill 1948 yield function.

F	G	H	N
0.63	0.67	0.33	1.46

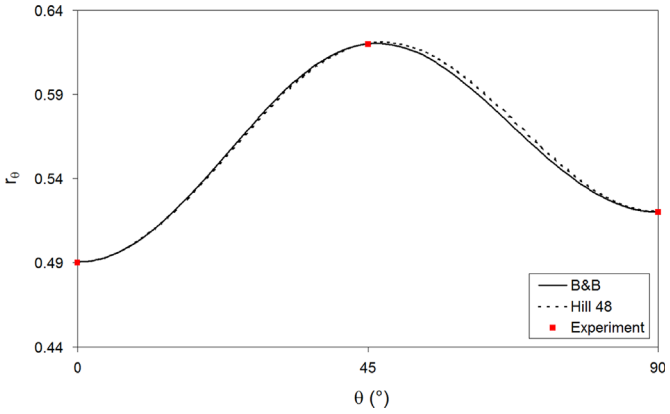

Fig. 3. Experimental and predicted anisotropic coefficients.

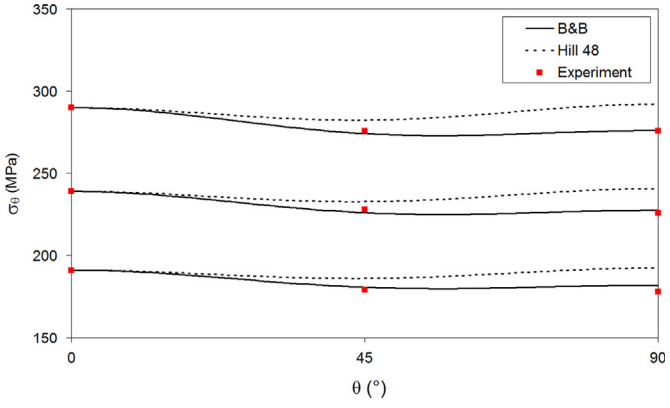

Fig. 4. Experimental and predicted uniaxial stresses.

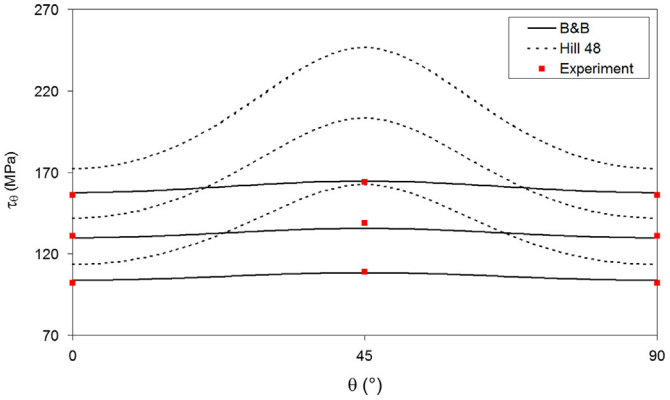

Fig. 5. Experimental and predicted shear stresses.

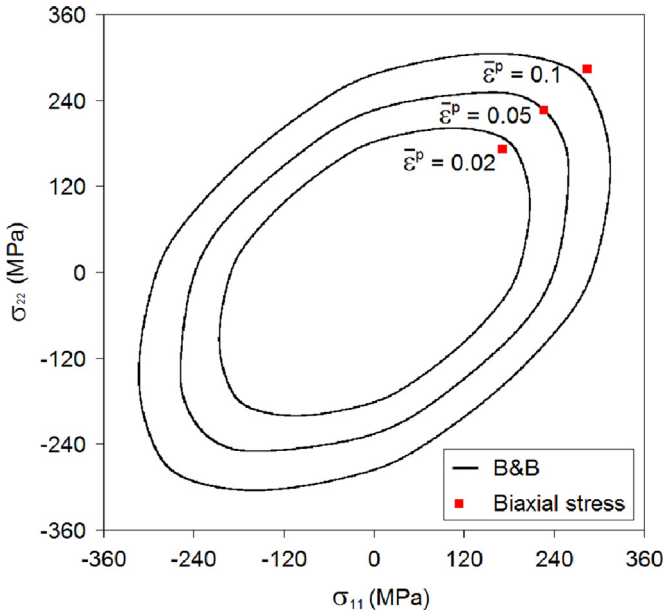

Fig. 6. Predicted yield surface contours.

4. Biaxial tensile test with cruciform specimen

4.1. Experiments

To simplify both the experimental database and the calibration of the yield function parameters, a second method based on data obtained from a cross biaxial tensile test was investigated. This test seems particularly interesting since different strain paths can be obtained simultaneously with a unique specimen [27].

A cruciform specimen shape has been designed and is shown in Fig. 7. Experiments on a servo-hydraulic testing machine have been performed (realized by LGCGM [28]) with a constant velocity ratio $v_x/v_y = 1$ imposed on four arms of the cruciform specimen;

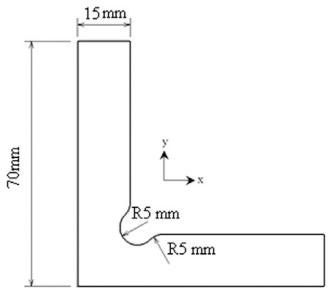

Fig. 7. Geometry of quarter cruciform specimen.

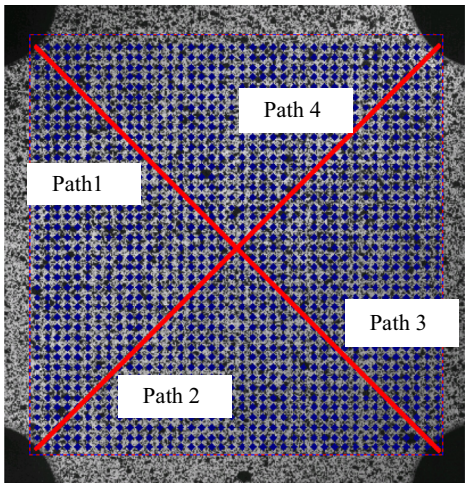

Fig. 8. Analysis section and visualization of the 4 diagonal paths.

$v_x = v_y = 1$ mm.s^{-1} are the imposed velocities along the arms of the sample (cf. Fig. 7 for the frame definition).

Images of the central area of the specimen are recorded with a high resolution camera and a digital image correlation software CORRELA 2D (developed by LMS at the University of Poitiers) is used to compute the in-plane strain components. As shown in Fig. 8, a central square area of approximately 25×25 mm^2 was selected, leading to a total number of about 1600 material points. Major strain ε_1 and minor strain $\varepsilon_2$were output at these material points and the strain path, characterized by the ratio $\varepsilon_2/\varepsilon_1$, was analyzed at time $t = 6.0$ s for a rupture time point recorded at time $t = 6.048$ s. Such a distribution is presented in Fig. 9. There is a nearly equi-biaxial stress state in the central area. It then changes gradually to nearly uniaxial tensile stress state at the corner. The maximum and minimum principal strains along four diagonal paths indicated in Fig. 9 have been compared in Figs. 10 and 11, respectively. The results obtained for the four paths are similar, whatever the selected path. A slight discrepancy is recorded near the free edge of the sample, the maximum relative gap being 1.7% for the major strain and 0.58% for the minor strain. An average value, both for minor and major strains, was then calculated over the four paths. This average is used in the following parts for the comparison with finite element simulation and identification procedure.

Fig. 12 shows the evolution of the loads recorded along the two arms: F_x and F_y. The rolling direction of the sheet corresponds to the x direction of the specimen. Due to the anisotropy, a difference can be observed between the two signals.

4.2. Numerical simulation

Finite element (FE) simulations of the biaxial test have been carried out with the commercial software ABAQUS, with the implicit solver. The anisotropic behavior of the material is modeled by Bron and Besson yield function implemented through a user subroutine. It should be emphasized that, as a first step, only anisotropy is dealt with.

Hardening of the material is modeled by isotropic hardening identified from a tensile test in the rolling direction. From the tensile test data in the rolling direction, and assuming isotropy, the equivalent plastic strain was calculated and Cauchy stress versus

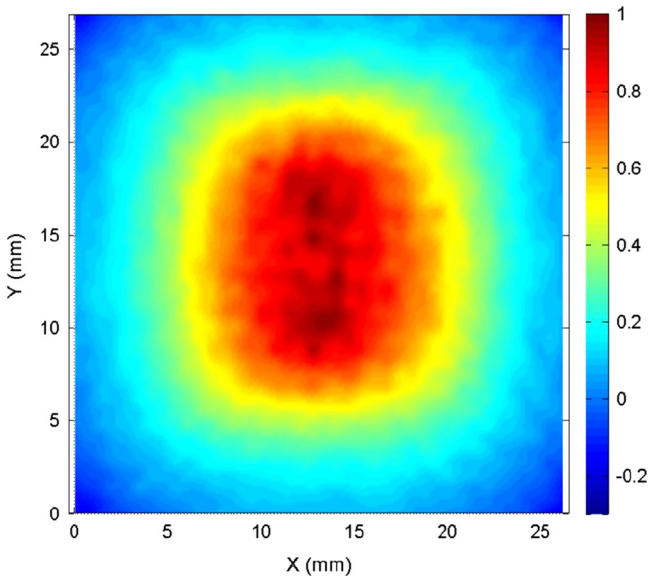

Fig. 9. Strain path ratio distribution $\varepsilon_2/\varepsilon_1$ in the analyzed central section.

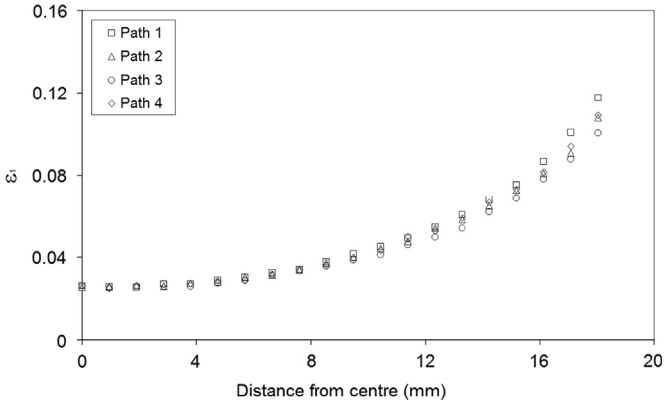

Fig. 10. Maximum principal strain along the four diagonal paths.

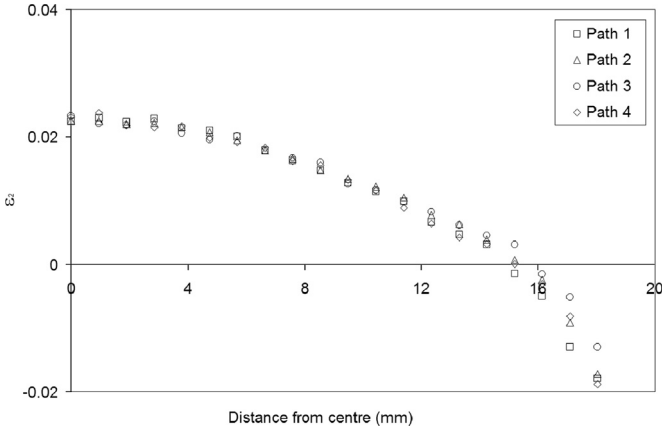

Fig. 11. Minimum principal strain along the four diagonal paths.

equivalent plastic strain curve was fitted with Voce equation $\sigma_0 = \sigma_s + Q(1-e^{-B\bar{\varepsilon}^p})$, with $\sigma_s = 146MPa$, $Q = 217.6MPa$ and $B = 10.9$. These parameters were determined from tensile data and were kept constant throughout the study. From the relation $\overline{\sigma} = Y_0$, it comes that the hardening law introduced in the finite element code is written as

$$\overline{\sigma} = \psi\left(\frac{[\sigma_{ij}]_{UT}}{\sigma_0}, a, b_1, b_2, \alpha^1, c_i^k\right)(\sigma_s + Q(1-e^{-B\bar{\varepsilon}^p})) \quad (13)$$

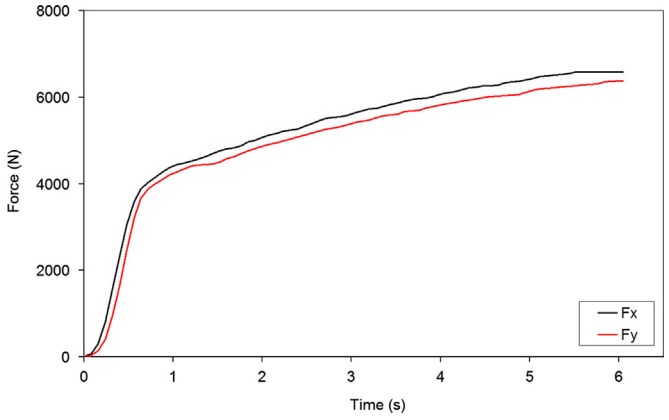

Fig. 12. Evolution of loads on the two arms.

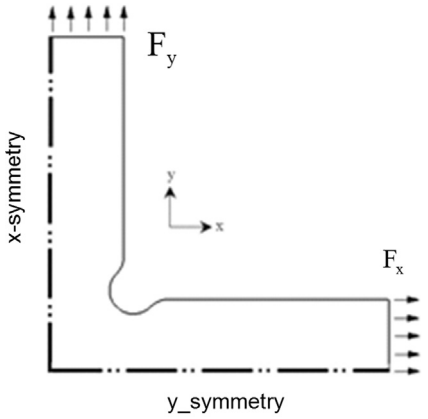

Fig. 13. FE boundary conditions.

where the first term in the right-hand side part of Eq. (13) depends only on the stress tensor for uniaxial tension in RD (only one non-zero component) normalized by the yield stress in RD and on the parameter set for the anisotropic yield criterion.

Due to the symmetry of the problem, only a quarter of the specimen is modeled. Experimental forces F_x and F_y given in Fig. 13 are imposed on the two arms of the cruciform specimen during the simulation process. Four node shell elements were used for the mesh, with a minimum size of 1 mm. Influence of the mesh size was investigated, in particular its influence on the major and minor strains, and stable predictions (accuracy of the same order that the one of experimental data) were obtained with the selected mesh. The computational time is about ten minutes (processor i7-640M (2.8 GHz) with 4 Go RAM) with these conditions.

The numerical simulation of biaxial tensile test has been performed with Bron and Besson and Hill 1948 yield criteria identified with conventional tests. Fig. 14 gives the equivalent plastic strain distribution in the central area of the specimen obtained at $t = 6.0$ s with Bron and Besson model. In order to analyze the evolution of the principal strains, a partition of the cruciform specimen in the central area has been performed along the diagonal direction and the values at the nodes along the partition line are output. The predicted principal strains and strain path ratio have been compared with the experimental results and are shown in Fig. 15(a–c). It can be seen that Bron and Besson predictions are close to the experimental results, while the values predicted by Hill 1948 criterion stand farther, especially for the minimum principal strain. Thus it is shown that the strain distribution in the center of the cruciform specimen is significantly dependent on the yield criterion. Bron and Besson parameter set identified with conventional tests has the capability to well describe the strain distribution, whereas Hill 1948 leads to significant discrepancies.

5. Parameter identification with biaxial tensile test data

Following the previous conclusion, that the strain distribution in the central area of the cruciform shape is sensitive to the yield criterion, identification of the material parameters based on the minimization of the gap between the evolution of major and minor strains along a diagonal path is performed in this section. Bron and Besson yield model is used in the numerical simulation of the biaxial tensile test.

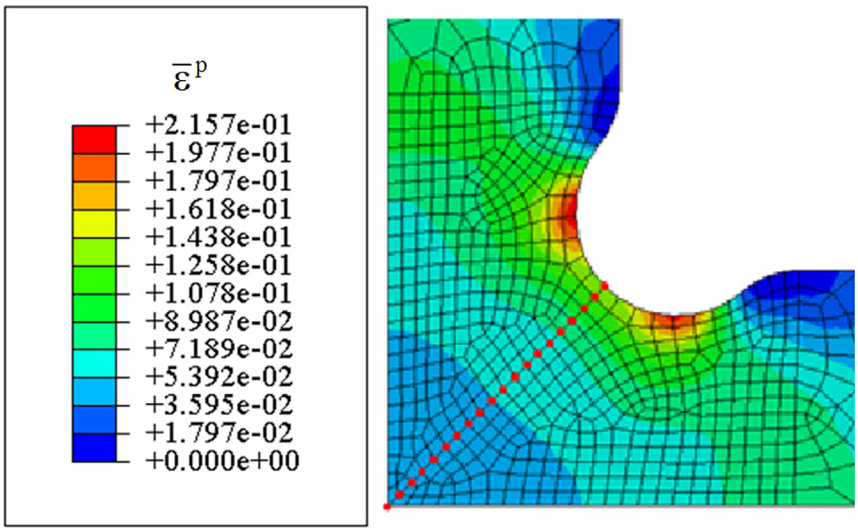

Fig. 14. Predicted equivalent plastic strain distribution and definition of the nodes along the diagonal direction used for the output.

A cost function is now defined to calculate the difference between the experimental and numerical principal strains

$$\delta_b(Y_0, a, b_1, b_2, \alpha^1, c_i^k) = \sum_{i=1}^{p} \left(\frac{\varepsilon_1^{EFi} - \varepsilon_1^i}{\varepsilon_1^i} \right)^2 + \sum_{i=1}^{p} \left(\frac{\varepsilon_2^{EFi} - \varepsilon_2^i}{\varepsilon_2^i} \right)^2 \quad (14)$$

where experimental values ε_1 and ε_2 are compared to the numerical values ε_1^{EF} and ε_2^{EF}. The index p in Eq. (14) stands for the number of points along the diagonal path. As the nodes used to output the strain components are different in the model and in the experiments, a linear interpolation of the experimental signals was performed. The minimization of the cost function is then performed with the software modeFRONTIER® which makes a coupling between ABAQUS and MATLAB. The algorithm SIMPLEX is preferred in the identification process. In an optimization procedure involving finite element integrations with many parameters and long calculation times for each iteration, the SIMPLEX is well adapted. For a set of 13 parameters, the algorithm needs 14 initial sets, which are randomly chosen in the variation range of the parameters. These sets permit to efficiently cover the space of solutions. It can be emphasized that the initial parameter sets for this identification, compared to the identification with conventional tests, are very different. The variation range of each parameter is the same as the one used for the conventional tests and is given in Table 2.

During the optimization process, the principal strain field at time $t = 6.0$ s is considered both in the experiments and in the numerical simulation. Table 5 gives the values of the newly identified parameters of Bron and Besson yield model after nearly 300 iterations.

Fig. 16(a) shows the predicted and experimental major and minor strain evolution along a diagonal path. According to this figure, there is a very good agreement between experiments and numerical simulation. The strain path ratio along the diagonal direction has been compared with the experimental one in Fig. 16(b). Bron and Besson model gives a slight underestimation at the beginning of the curve (central area of the cruciform specimen). However, farther from the center, the prediction is rather close to the experiments.

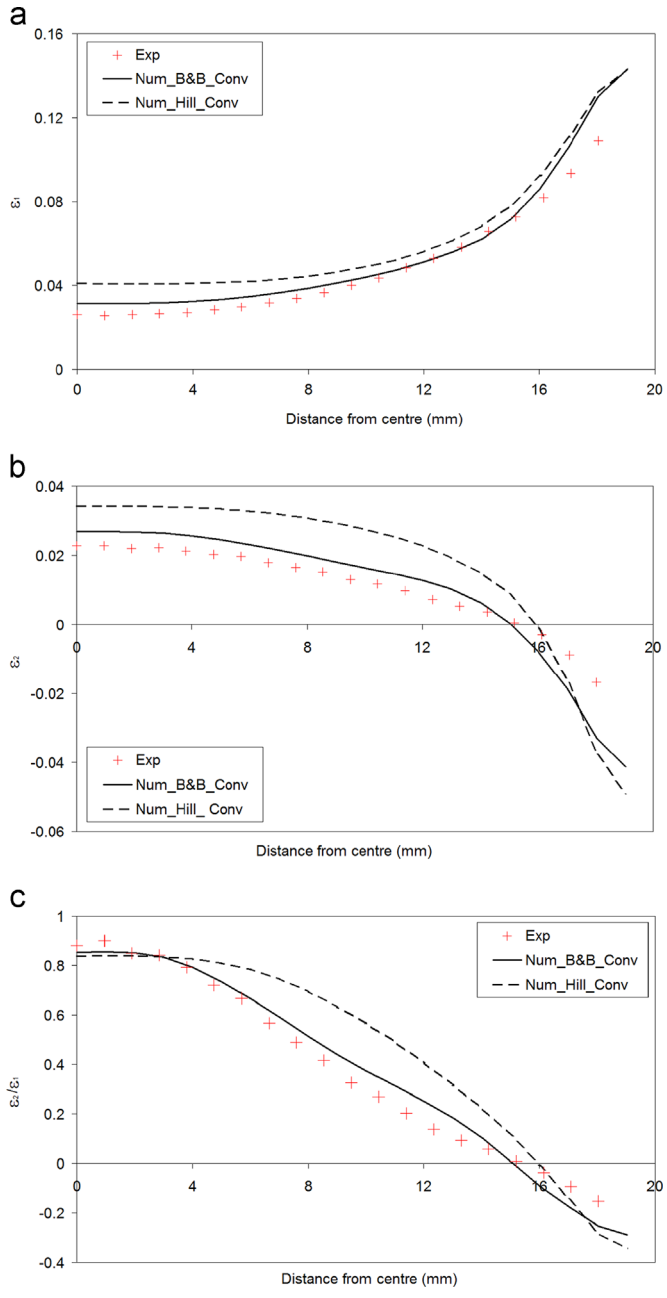

Fig. 15. (a) Major strain, (b) minor strain and (c) strain path ratio.

6. Comparison of the two methods

Both methods involve mechanical tests with DIC local strain measure. However, in the case of conventional tests, the strain field can be confidently considered homogeneous, e.g. for simple shear test and an average shear strain γ of 0.3, a maximum relative gap of $\pm 5\%$ was recorded, related to the accuracy of the strain measure [6]. This value is significantly lower than the strain range recorded in biaxial test, with an equivalent strain that ranges from 0.02 up −0.12. Moreover, there is almost no strain path ratio variation over the selected areas for conventional tests whereas it evolves significantly for the biaxial test.

The experimental data represented in the plane $(\varepsilon_2, \varepsilon_1)$ corresponding to both the conventional tests and the biaxial test used in the identification procedure are shown in Fig. 17. For the first method, the sampling points occupy a larger area in the plane $(\varepsilon_2, \varepsilon_1)$ however the information is more discrete when compared to the approach with only the biaxial test. Indeed, a large number of strain path ratios are then investigated, though for a fixed strain level. A possibility to enrich this database would be to add other path than the diagonal one or use the same path but at different strain levels.

Fig. 18 shows the predicted conventional tests with parameter set of Table 5. It can be seen that the overall trend and level are well respected for each type of test. Indeed, stress level in bulge test is well predicted up to an equivalent plastic strain of 0.2 as well as for simple shear test at 45°/RD. However, some discrepancies are evidenced. Indeed, no variation for the shear stress, whatever the orientation to the rolling direction, was predicted

Table 5
Anisotropic parameters of Bron and Besson yield function identified by biaxial test.

$Y_0(MPa)$	α_1	a	b_1	b_2	c_1^1	c_2^1	c_3^1	c_4^1	c_1^2	c_2^2	c_3^2	c_4^2
125.9	0.72	0.16	13.00	8.41	1.06	1.10	0.82	0.95	0.75	0.47	0.78	0.62

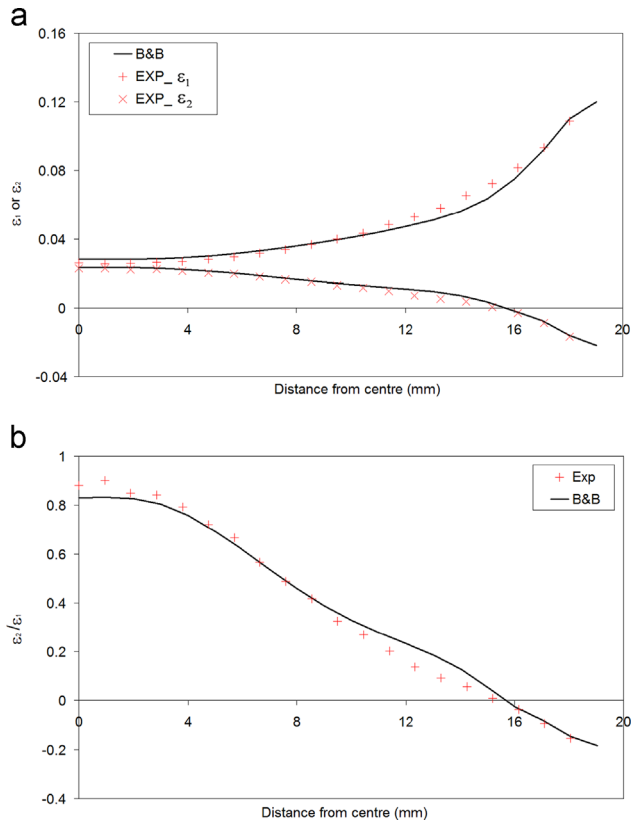

Fig. 16. (a) Principal strains predicted by Bron and Besson yield function with parameters identified from the biaxial test. (b) Strain path ratio predicted by Bron and Besson yield function with parameters identified from the biaxial test.

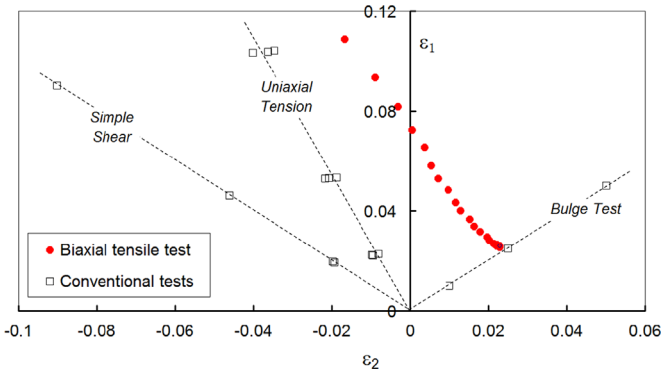

Fig. 17. Strain paths for the two identification methods.

though it comes from experiments that the shear stress along RD is lower than the one at 45°/RD. Concerning the uniaxial tensile tests, though the stress level in RD is above the ones in 45° and 90° to RD in the experiments, a different tendency is predicted, with stress at 0° and 45° to RD well above the one at 90°/RD. It seems therefore that the uniaxial stress state is not well enough represented in the series of stress states along the diagonal direction for the biaxial test. Further work is under progress with taking into account other paths like longitudinal and transverse paths to output the strain data.

Fig. 19 gives a comparison between two yield contours calculated with parameters of Bron and Besson model obtained either from conventional tests or the biaxial test. There is only a small difference between these two contours, mainly near the plane strain state.

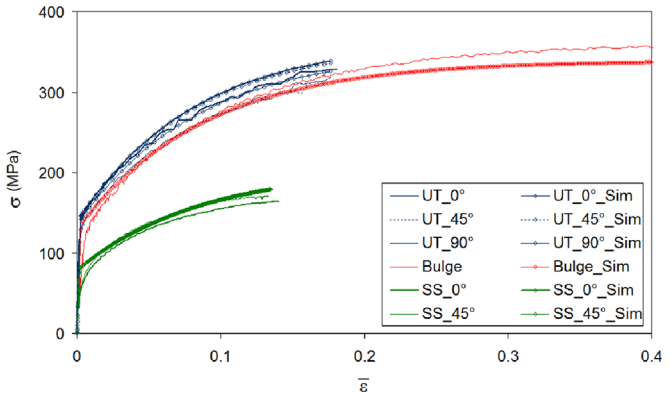

Fig. 18. Prediction of stress–strain curves for conventional tests using parameter set (Table 5) identified from the biaxial test.

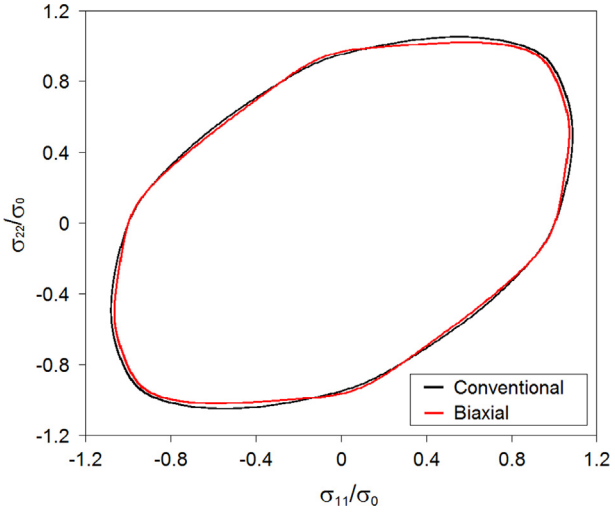

Fig. 19. Comparison of two yield contours.

7. Conclusion

Bron and Besson yield model has been used to predict the anisotropic behavior of material AA5086. 13 parameters of the yield model have been identified by two different methods. The first method is associated with conventional homogeneous tests: uniaxial tension, biaxial tension by hydraulic bulging and simple shear. To take into account the subsequent evolution of anisotropy, the identification process is performed with the material data at several plastic strains. The other method is based on only a biaxial test realized on a cruciform specimen. The identification is carried out with a comparison of experimental and numerical principal strains along a diagonal direction of the specimen central area. It is shown that (i) the numerical prediction of the principal strains is significantly dependent on the yield model (Bron and Besson and Hill 1948) and that (2) the two methods give similar yield contours, except near the plane strain state. Finally, it can be concluded that a single biaxial tensile test seems sufficient to obtain all the material parameters of a complex yield criterion for AA5086 sheet.

Acknowledgments

S. Zang appreciates the partial support by the National Natural Science Foundation of China (No. 11002105). D. Guines, L. Léotoing, S. Thuillier are grateful for the financial support from RTR Bresmat

2013 of Université européenne de Bretagne. S. Zhang thanks for the financial support of China Scholarship Council.

References

[1] Hill R. A theory of the yielding and plastic flow of anisotropic metals. Proc R Soc Lond Ser A: Math Phys Sci 1948;193:281–97.
[2] Barlat F, Brem JC, Yoon JW, Chung K, Dick RE, Lege DJ, et al. Plane stress yield function for aluminum alloy sheets—Part 1: theory. Int J Plast 2003;19:1297–319.
[3] Barlat F, Aretz H, Yoon JW, Karabin ME, Brem JC, Dick RE. Linear transfomation-based anisotropic yield functions. Int J Plast 2005;21:1009–39.
[4] Karafillis AP, Boyce MC. A general anisotropic yield criterion using bounds and a transformation weighting tensor. J Mech Phys Solids 1993;41:1859–86.
[5] Banabic D. Sheet metal forming processes: constitutive modeling and numerical simulation. Heidelberg Dordrecht London New York: Springer; 2010.
[6] Zang SL, Thuillier S, Le Port A, Manach PY. Prediction of anisotropy and hardening for metallic sheets in tension, simple shear and biaxial tension. Int J Mech Sci 2011;53:338–47.
[7] Suh YS, Saunders FI, Wagoner RH. Anisotropic yield functions with plastic-strain-induced anisotropy. Int J Plast 1996;12:417–38.
[8] Zang S, Lee M. A general yield function within the framework of linear transformations of stress tensors for the description of plastic-strain-induced anisotropy. AIP Conf Proc 2011;1383:63–70.
[9] Barlat F, Lege DJ, Brem JC. A six-component yield function for anisotropic materials. Int J Plast 1991;7:693–712.
[10] Aretz H. A non-quadratic plane stress yield function for orthotropic sheet metals. J Mater Process Technol 2005;168:1–9.
[11] Aretz H. Applications of a new plane stress yield function to orthotropic steel and aluminium sheet metals. Model Simul Mater Sci Eng 2004;12:491–509.
[12] Aretz H, Hopperstad OS, Lademo O-G. Yield function calibration for orthotropic sheet metals based on uniaxial and plane strain tensile tests. J Mater Process Technol 2005;186:221–35.
[13] Bron F, Besson J. A yield function for anisotropic materials Application to aluminum alloys. Int J Plast 2004;20:937–63.
[14] Banabic D, Aretz H, Comsa DS, Paraianu L. An improved analytical description of orthotropy in metallic sheets. Int J Plast 2005;21:493–512.
[15] Comsa D, Banabic D. Plane-stress yield criterion for highly-anisotropic sheet metals. In: Proceedings of the 7th International conference and workshop on numerical simulation of 3D sheet metal forming processes, NUMISHEET 2008. Interlaken, Switzerland; 2008. p. 43–8.
[16] Hu W. Constitutive modeling of orthotropic sheet metals by presenting hardening-induced anisotropy. Int J Plast 2007;23:620–39.
[17] Barros PD, Oliveira MC, Alves JL, Menezes LF. Earing prediction in drawing and ironing processes using an advanced yield criterion. Key Eng Mater 2013;554–557:2266–76.
[18] Cazacu O, Barlat F. Generalization of drucker's yield criterion to orthotropy. Math Mech Solids 2001;6:613–30.
[19] Wang H, Wan M, Wu X, Yan Y. The equivalent plastic strain-dependent Yld2000-2d yield function and the experimental verification. Comput Mater Sci 2009;47:12–22.
[20] Green DE, Neale KW, MacEwen SR, Makinde A, Perrin R. Experimental investigation of the biaxial behaviour of an aluminum sheet. Int J Plast 2004;20:1677–706.
[21] Teaca M, Charpentier I, Martiny M, Ferron G. Identification of sheet metal plastic anisotropy using heterogeneous biaxial tensile tests. Int J Mech Sci 2010;52:572–80.
[22] Ferron G, Makkouk R, Morreale J. A parametric description of orthotropic plasticity in metal sheets. Int J Plast 1994;10:431–49.
[23] Prates PA, Fernandes JV, Oliveira MC, Sakharova NA, Menezes LF. On the characterization of the plastic anisotropy in orthotropic sheet metals with a cruciform biaxial test. IOP Conf Ser Mater Sci Eng 2010;10:012142.
[24] Heath MT. Scientific computing, an introductory survey. 2nd ed.. New York: McGraw-Hill; 2002.
[25] Information on ⟨http:/www.esteco.com/modefrontier⟩.
[26] Woodthorpe J, Pearce R. The anomalous behaviour of aluminium sheet under balanced biaxial tension. Int J Mech Sci 1970;12:341–7.
[27] Kuwabara T, Ikeda S, Kuroda K. Measurement and analysis of differential work hardening in cold-rolled steel sheet under biaxial tension. J Mater Process Technol 1998;80–81:517–23.
[28] Zidane I, Guines D, Leotoing L, Ragneau E. Development of an in-plane biaxial test for forming limit curve (FLC) characterization of metallic sheets. Meas Sci Technol 2010;21:055701.